Chemical Science

Accepted Manuscript

This article can be cited before page numbers have been issued, to do this please use: A. R. LeBlanc, J. R. Smith, A. J. Isakov, J. Bacsa and W. Wuest, *Chem. Sci.*, 2026, DOI: 10.1039/D6SC04046B.

ROYAL SOCIETY OF CHEMISTRY

rsc.li/chemical-science

View Article Online
DOI: 10.1039/D6SC04046B

ARTICLE

Concise Synthesis of Simplified Aogacillin Analogs Reveals Innate Reactivity and Synergy with Aminoglycosides

Received 00th January 20xx,
Accepted 00th January 20xx

DOI: 10.1039/x0xx00000x

Andrew R. LeBlanc[a], Jacqueline R. Smith[a], Audrey J. Isakov[a], John Bacsa[a], William M. Wuest[a]*

ABSTRACT: Aogacillins (AOGs) A-B, two diastereomeric natural products isolated from *Simplicillium* sp. FKI-5985, were reported to have potent synergism with aminoglycoside antibiotics. Herein, we show that structural simplification expedites the synthesis of AOG analogs in 3-4 steps. Further, we demonstrate that these compounds irreversibly trap cysteine nucleophiles at an electrophilic enone warhead but are also susceptible to [4+2] cycloadditions. Therefore, strategically designed AOG analogs were constructed to mitigate side reactivity and sensitize MRSA to aminoglycosides at sub-MIC concentrations.

Introduction:

Natural products (NPs) are uniquely privileged in the realm of antibiotics, with over 65% of FDA approved antibiotics being NPs or NP-derived.[1] Historically, NPs such as vancomycin, linezolid, and gentamicin act as a frontline defense for gram-positive bacteria, including methicillin-resistant *Staphylococcus aureus* (MRSA), however, continued resistance to these therapeutics is pressing. The United States Center for Disease Control (CDC) classifies MRSA as a serious threat with over 80,000 severe infections in the United States each year.[2,3,4] Taken together, there is a significant urgency for the community to develop new approaches to tackle antimicrobial resistance (AMR).

There are two main avenues through which NPs can combat AMR. They can possess novel mechanisms of action (MOAs) not used in the clinic, thereby limiting the likelihood of being predisposed, as bacteria may not have evolved mechanisms against them. For example, lefamulin is a pleuromutilin-derived NP that targets the bacterial peptidyl transferase center on the 50S subunit of the ribosome and was first approved by the FDA in 2019.[5,6] Its novel MOA and short time in the clinic has resulted in low levels of reported resistance.[7] Alternatively, NPs can sensitize bacteria to previously approved antibiotics by targeting the resistance mechanism itself.[8] This approach was the foundation for the FDA-approved combination therapy Avycaz™, composed of ceftazidime/avibactam. Ceftazidime is a third-generation β-lactam which was FDA approved in 1985 but shortly became ineffective due to the overexpression of β-lactamase enzymes.[9] Avibactam, a β-lactamase inhibitor, targets the enzyme responsible for ceftazidime resistance, therefore, when used in combination, ceftazidime/avibactam regains its efficacy.

Aided by thousands of years of evolutionary pressure, antimicrobial NPs have diverse biological activity. Aogacillins (AOGs) A-B, isolated in 2013 from *Simplicillium* sp. FKI

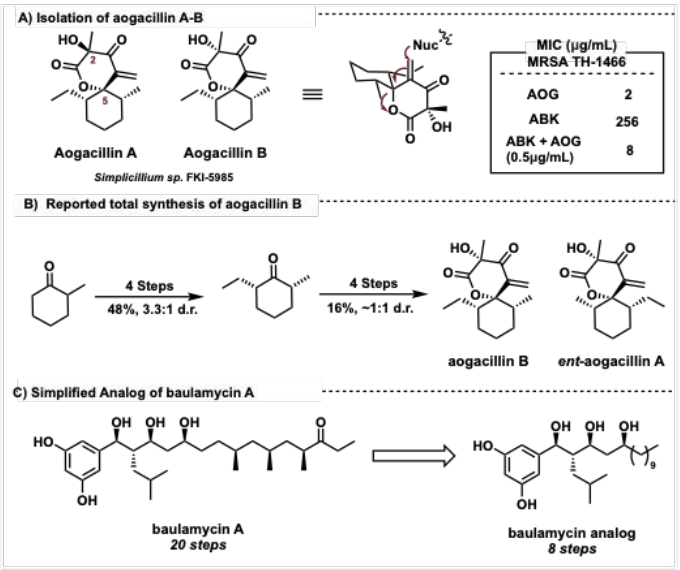

Figure 1: A) Aogacillin A-B and reported biological activity. **B)** Zhang's total synthesis of AOG B and ent-AOG A. **C)** Simplified analog of baulamycin A.

[a] Department of Chemistry, Emory University, Atlanta, GA, 30322, United States

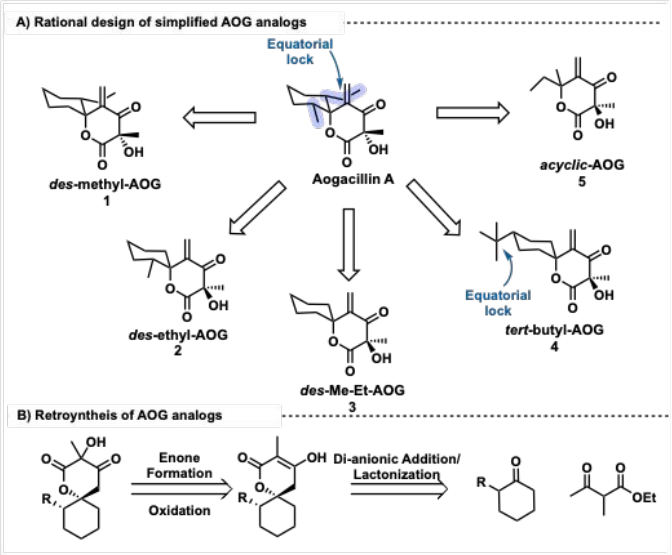

Figure 2: **A)** Rational design of AOG simplified analogs. **B)** Retrosynthetic approach for AOG analogs.

5985, are diastereomeric NPs only differing in the relative stereochemistry of the tertiary alcohol (**Figure 1a**).[10] Furthermore, AOG A-B were reported to have a minimum inhibitory concentration (MIC) of 2 μg/mL against MRSA. Interestingly, AOG A-B were also found to sensitize aminoglycoside-resistant MRSA to arbekacin (ABK) at sub-MIC concentrations, lowering the MIC of ABK from 256 to 8 μg/mL.[10] The biological activity, coupled with its unique chemical structure, has made AOG a desirable synthetic target. In 2026, Zhang, Tong, and co-workers published the first total synthesis of aogacillin B and *ent*-aogacillin A in 8 steps and 5% overall yield.[11] Their route highlights a strategic aldol and lactonization sequence to both install the tertiary alcohol and close the spirocycle in one step (**Figure 1b**).

We became interested in AOG for its biological activity and hypothesized that a simplified analog would be both viable and useful. We realized that the exocyclic enone is likely the molecular warhead, able to accept biological nucleophiles, contributing to its MOA. Unlike common electrophilic warheads, AOG possesses a *β*-leaving group (**C5** carboxylate) that could be expelled after Michael addition, leading to an irreversible covalent adduct (**Figure 1a**).

As such, we proposed that the exocyclic enone/spirocyclic motif was the main pharmacophore responsible for its biological activity and set out on a campaign to design analogs around this scaffold.

Examining AOG A-B from a retrosynthetic perspective, we identified that the main synthetic hurdle was not the spirocycle/enone motif, but the unique methyl/ethyl substitution pattern. In the case of Zhang's total synthesis, four steps were used to install the ethyl group.[11] As such, we hypothesized that deletion of the methyl and/or ethyl group could drastically decrease the synthetic burden while still accessing the same chemical space and maintaining biological activity.

Our group and others have had a successful track record leveraging NP simplification.[12–17] One specific example relates to the anti-MRSA NP baulamycin A whose total synthesis took 20 total synthetic steps, whereas the simplified analogs only took 8 (**Figure 1c**). Furthermore, the simplified analogs displayed a decreased MIC against *S. aureus*.[18] With this approach in mind, we set out to synthesize and biologically evaluate simplified AOG analogs.

Initially, we imagined deletion of the methyl and/or ethyl groups would provide three analogous compounds: *des*-methyl-AOG **1**, *des*-ethyl-AOG **2**, and *des*-methyl-ethyl-AOG **3** (**Figure 2a)**. Conformationally, however, the methyl/ethyl groups are both equatorial, locking the resulting chair conformation, which we speculated is critical for the biological activity. Therefore, many of our designs sought to preserve this key structural feature. For example, installing a remote *tert*-butyl group would similarly lock the chair conformation **4**. Lastly, we envisioned removing the spirocyclic nature of the scaffold altogether to access an acyclic analog, **5**. Retrosynthetically, access to the core scaffold could be forged via a di-anionic addition-lactonization sequence to efficiently install the spirocycle, an alternative approach in comparison to Zhang.[11] From this advanced intermediate, subsequent oxidation of the enone to the tertiary alcohol and methylene installation would provide rapid access to the simplified AOG scaffold (**Figure 2b**).

Results and Discussion:

We initially targeted *des*-methyl-ethyl **3** and began with the di-anionic addition of ethyl-2-methylacetoacetate to cyclohexanone to afford the desired 1,2-addition. Subsequent treatment with NaOH resulted in lactonization to form **5** in 45% yield over the sequence (**Figure 3**). To access the first AOG analog we needed to 1) oxidize **C2** to the tertiary alcohol and 2) install the **C4** exocyclic enone. With those transformations in mind, we screened a variety of oxidants (**SI Table 1-3)** and found that magnesium bis(monoperoxyphthalate) with $NaHCO_3$ in aqueous methanol

View Article Online
DOI: 10.1039/D6SC04046B

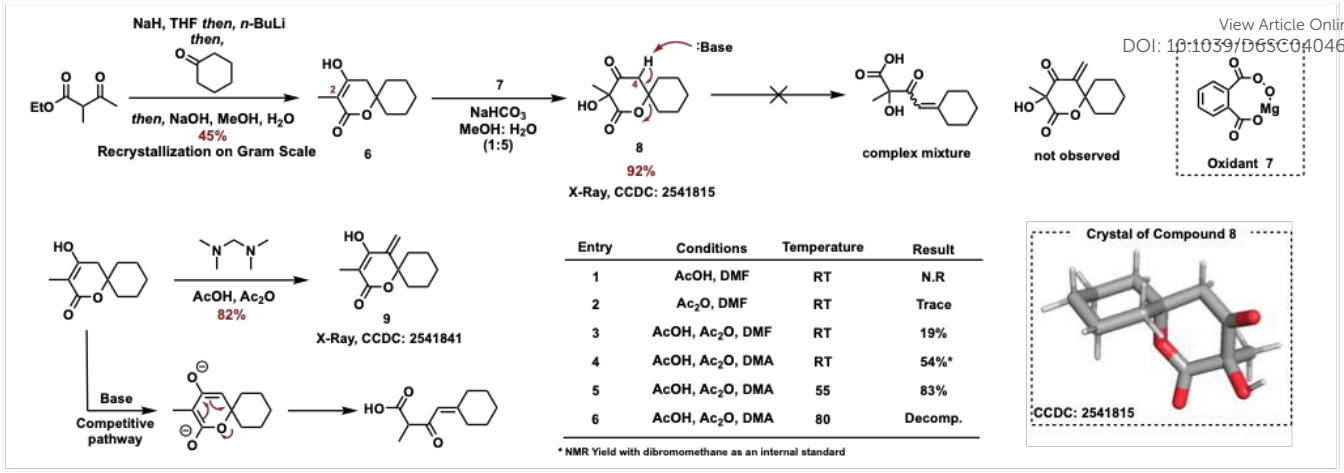

Figure 3: Synthetic route towards des-Me-Et-AOG and exocyclic alkene optimization.

cleanly provided **8** (92%; confirmed by X-ray crystallography, CCDC: 2541815). Omission of base or increased methanol concentrations were deleterious to the reaction (**SI Figure 1**). Installation of the exocyclic alkene also proved challenging. Utilization of various formaldehyde surrogates, under several conditions proved unsuccessful. Instead, we observed irreversible elimination of the lactone as deprotonation at **C4** enables rapid E1cB elimination, which outcompetes the desired condensation.

To overcome this, we first installed the enone and then oxidized the core scaffold. Again, this unique spirocyclic core at the *β*-position made alkene installation difficult as competing elimination reopened the spirocycle. However, after multiple rounds of optimization (**SI Tables 4-6)**, we found that treatment of **6** with *N,N,N,N'*-tetramethyldiaminomethane, acetic acid and acetic anhydride in DMA resulted in formation of the exocyclic enone (**Figure 3, Optimization Table).** With the enone installed we set out to perform the last oxidation. Surprisingly, initial attempts at oxidation were unsuccessful and either resulted in recovered starting material or a complex mixture of dimers (**SI Table 7**). Concurrently, we were also investigating the synthesis of compounds **1** and **2**, which underwent the same di-anionic

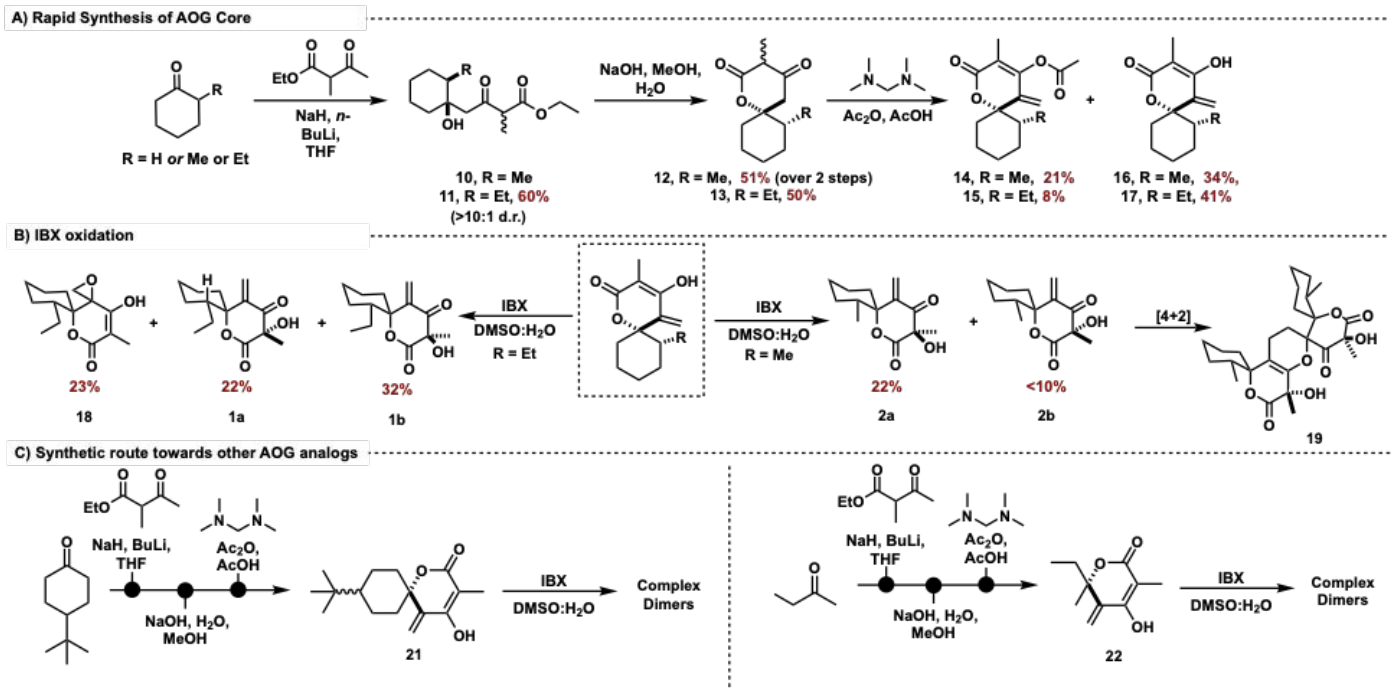

Figure 4: **A)** Synthesis towards the core of des-Me-AOG, des-Et-AOG, and des-Et-Me-AOG. **B)** IBX oxidation to access des-Me-AOG and des-Et-AOG. **C)** Synthesis towards the core of tert-butyl-AOG and acyclic-AOG.

View Article Online
DOI: 10.1039/D6SC04046B

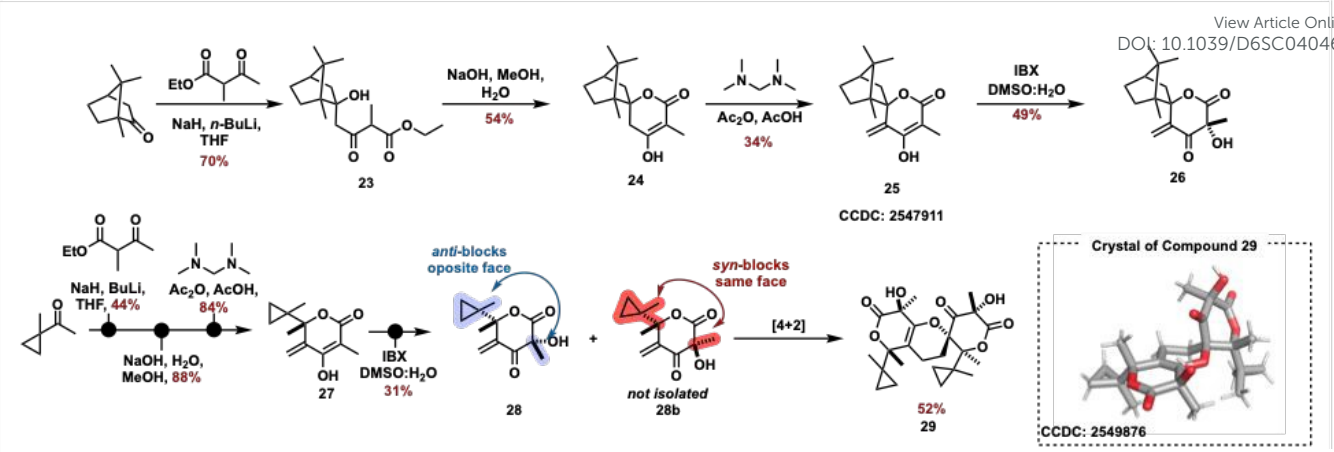

Figure 5: Synthesis of sterically hindered AOG analogs to prevent dimerization.

addition followed by subsequent lactonization to form the spirocyclic core. We were able to confirm the relative stereochemistry of **12** via X-ray crystallography (CCDC: 2543179). Treatment of both **12** and **13** under the optimized enone formation conditions resulted in formation of **16** and **17** respectively (**Figure 4a**). We also found side formation of the acetyl-protected enone, **14** and **15.** These results demonstrate the robust nature of this method which could lend itself to other applications for the installation of exocyclic enones with β–leaving groups.

Toward the completion of simplified AOG analogs, treatment of **17** with IBX provided conversion to both diastereomers of *des*-methyl-AOG (**1a**, 22%; **1b**, 32%). We also isolated **18** as a minor side product resulting from epoxidation across the exocyclic alkene. These same conditions work well with **16,** providing both diastereomers of *des*-ethyl-AOG in 40% and <10%. Interestingly, we attribute the poor yield of **2b** to an alternate reactivity profile, where it undergoes an oxa-Diels Alder cycloaddition to form **19**.

We attribute this selectivity between **2a** and **2b** to the *syn*-relationship between the methyl and α-methyl groups in **2b,** whereby this relationship blocks the front face of the compound leaving the back face sterically accessible for the cycloaddition (**Figure 4b**). Alternatively, **2a** possesses an *anti*-relationship between the methyl and α-methyl group, each blocking differing faces of the enone, preventing the [4+2] cycloaddition and providing the scaffold with a privileged reactivity profile. Furthermore, the relative regiochemistry of this dimer was unexpected and counterintuitive, with the enone reacting at the α-position rather than the expected, and polarity matched, β-position. We found that this regiochemistry is reported in other NP dimerizations. (**SI Figure 3**).[19,20,21] Attempts to take this unique side product and undergo a retro-[4+2] cycloaddition were explored but resulted in decomposition. We also saw evidence for dimerization with compounds **21** and **22,** however, the lack of substitution resulted in a non-diastereoselective [4+2] and a complex mixture of diastereotopic dimers (**SI Figure 4**) (**Figure 4c**). Of note, we found that no AOG dimer has ever been reported or commented on. Taken together, we hypothesize that the remote methyl and ethyl substituents in the NP likely provide steric interference, thereby decreasing its propensity to dimerize.

Steric Analogs:

Due to the prevalence of oxa-Diels Alder dimeric natural products, we rationalized that the propensity for dimerization was not only a chemical liability but may also dimerize under biological conditions. As such, we aimed to synthesize new AOG inspired analogs with increased sterics to prevent dimerization. We first selected a camphor derivative due to it rigid and sterically demanding core. Furthermore, the natural concavity of camphor would direct the first di-anionic addition to the convex face and result in the exocyclic alkene being buried in the convex face of the scaffold. Taking camphor through the di-anionic addition, lactonization, and alkene installation we accessed **25** in 4 steps (confirmed via X-ray, CCDC: 2547911). Treatment of **25** with IBX proceeded smoothly to give the oxidized derivative in 49% yield (5.7:1 d.r.). Importantly, we found no evidence of dimerization, further highlighting the role of remote sterics (**Figure 5**).

Next, we designed a cyclopropyl analog, **27**, that would juxtapose **22.** We rationalized that the increase in sterics might be enough to prevent the dimerization. To this end, we synthesized a cyclopropyl analog, **27,** in three steps. Excitingly, we found that **27** readily undergoes IBX oxidation; however, one diastereomer (**28b**) dimerizes to **29** (confirmed by X-ray, CCDC: 2549876). Comparable to **2a-b**, we attribute this selectivity to the *syn*-relationship between the cyclopropyl

and methyl group whereby the back face is accessible for the cycloaddition.

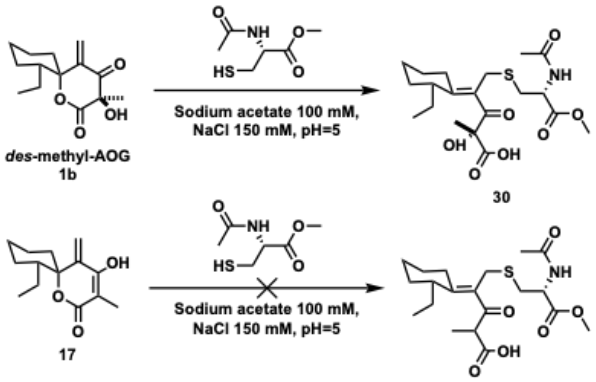

Figure 6: Covalent reactivity of des-methyl-AOG and **17.**

Covalent reactivity:

With a series of AOG analogs in hand, we wanted to test our initial hypothesis that the enone and spirocycle acted as an irreversible covalent trap. To investigate the chemoselectivity of AOG analogs, compound **1b** was mixed with an equimolar ratio of Boc-Lys-OMe, Boc-Ser-OMe, and Ac-Cys-Ome, in pH 7.4 PBS buffer. After 10 min, the reaction was analyzed directly by LCMS (**SI Figure 5**). A mass adduct matching that of a covalent reaction with cysteine was the sole product identified. To determine the structure of the cysteine-bound adduct, the reaction was scaled up and probed over a range of pHs. At pH 5, the cleanest conversion was seen and the irreversibly bound adduct was isolated (**Figure 6**). In contrast, we found that treating **17** with Ac-Cys-OMe resulted in no reaction. We hypothesize that the lack of oxidation at the α-position allows for extended conjugation throughout the π-system of the exocyclic alkene, thus decreasing the electrophilicity of the enone itself. Qualitatively, examination of ^{1}H-NMR shows that the vinyl protons of **17** are drastically shielded in comparison to those on **1b**. The requirement to have oxidation at the α-position to permit covalent reactivity, coupled with the fact that the ethyl/methyl aid in preventing dimerization, suggests that this unique functionality may be a result of evolutionary refinement of the scaffold.

Biological Activity:

With synthetic analogs in hand, we set out to test the biological activity of these natural product-inspired compounds. We found that our synthetic derivatives showed poor activity against methicillin-resistant *S. aureus* (MRSA) on their own, with all MIC values exceeding 250 µM, in contrast to the reported data (**Figure 7a**). When analogs were treated in conjunction with aminoglycoside antibiotics against a resistant strain (ATCC43300), the analogs were found to restore aminoglycoside activity. Checkerboard assays reveal (R)-*des*-methyl-AOG (**1b**) to have synergy with arbekacin, which aligns with literature reports of the natural product activity.[10] The AOG analogs lowered doses from 20 µM to 2 µM (**Figure 7b**, (*R*)-*des*-methyl-AOG 63 µM, arbekacin 2 µM, FIC = 0.150; camphor-AOG 63 µM, arbekacin 2 µM, FIC = 0.201). Excitingly, synergy was also found between **1b** (125 µM) and gentamicin, a widely used aminoglycoside, granting a gentamicin MIC of 63 µM (FIC = 0.201) when this strain was previously resistant (MIC = 625 µM). Similarly, camphor-AOG (**26** at 125 µM) is synergistic with gentamicin, lowering the MIC from 625 to 32 µM (FIC = 0.251). These findings expand the synergistic scope of these simplified analogs through checkerboard synergy with aminoglycosides, while the activity of natural or fully synthetic aogacillin was not

A)

	MIC (µM) MRSA Strain	
	USA300	43300
des-Me-Et-AOG	>250	*N.T.*
(S)-des-Me-AOG	>250	*N.T.*
(R)-des-Me-AOG	>250	*N.T.*
(S)-des-Et-AOG	>250	*N.T.*
(R)-des-Et-AOG	>250	1,250
camphor-AOG	>250	625
Vancomycin	1	*N.T.*
Gentamicin	*N.T.*	625
Arbekacin	*N.T.*	20

B)

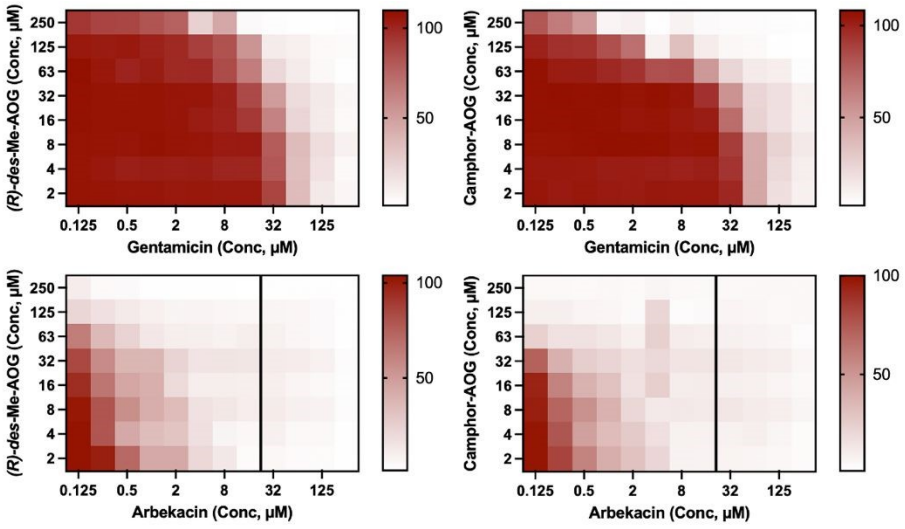

Figure 7: A) MICs of AOG analogs and antibiotics against MRSA USA3-0114 and MRSA ATCC43300. N.T. = not tested. **B)** Synergy heatmaps, % growth of MRSA ATCC43300 when treated with varying concentrations of AOG analog and aminoglycoside. All reported data are the average of 3 biological replicates.

directly evaluated. Future work will investigate the mechanism of this synergistic effect.

Conclusion:

At the outset of the project, we aimed to access a similar chemical space to AOG while decreasing the synthetic burden to access these compounds. Visually representing this idea of chemical space has been pioneered by Shenvi.[22,23] To exemplify our approach, we examined the structures of AOG, *des*-methyl-AOG, *des*-ethyl-AOG, and camphor-AOG and calculated their principal moment of inertia (I_1/I_3 and I_2/I_3) and the Bottcher complexity per atom (C_m/atom).[22,24] As expected, when graphed on a 3D plot, the AOG analogs occupy a similar region in chemical space (**Figure 8**).[23,25] We then plotted all synthetic compounds and intermediates (black line) of our approach alongside those for Zhang's total synthesis (red dotted line). Both our starting material and that for Zhang's synthesis originate in a similar area, thereby demonstrating how we can access the same region of chemical space in half the number of synthetic steps. That being said, our di-anionic route was unable to access AOG due to its inability to lactonize following the 1,2-addition. (**SI Figure 6**). This exemplifies how slight changes to the targeted chemical space can unlock alternative synthetic routes. Finally, we show that dimerization allows access to yet another region of chemical space we initially did not anticipate.

In conclusion, we have synthesized a series of AOG analogs that access the same chemical space as the corresponding NP in 3-4 synthetic steps. Throughout our synthetic approach we observe key structural features of this scaffold that impart privileged reactivity. For example, the methyl/ethyl substituents also appear to temper the side-reactivity of the off-pathway [4+2] dimerization of the enone itself. We also demonstrated how the unique spirocyclic enone motif reacts with cysteine and expels the carboxylate only when the α-oxidation is present. Taken together this work highlights the intricacies of the seemingly simple AOG scaffold and uncovers unique principles clearly harnessed by nature. These reactive structural features and key structural changes drastically reduce the synthetic complexity, enabling a concise synthesis of compounds that confer synergistic interactions with clinically relevant aminoglycoside antibiotics against resistant MRSA strains.

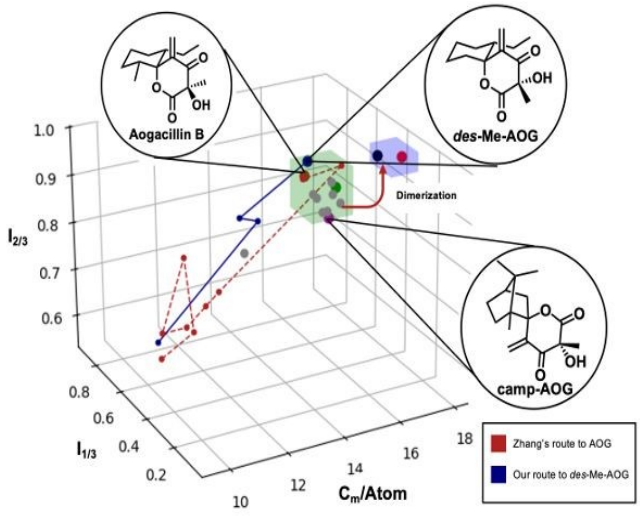

Figure 8: The chemical space of AOG, AOG analogs, overlayed with Zhang's route to AOG B and our route to des- methyl-AOG.

Author contributions

The manuscript was written through contributions of all authors. All authors have given approval to the final version of the manuscript.

Conflicts of interest

There are no conflicts to declare.

Data availability

The data underlying this study are available in the published article and its Supporting Information. Detailed experimental procedures, characterization data, and NMR spectra. Compound **8** corresponds to CCDC accession code 2541815. Compound **9** corresponds to CCDC accession code 2541841. Compound **12** corresponds to CCDC accession code 2543179. Compound **25** corresponds to CCDC accession code 2547911. Compound **29** corresponds to CCDC accession code 2549876.These data can be obtained free of charge via the joint Cambridge Crystallographic Data Centre (CCDC) and Fachinformationszentrum Karlsruhe Access Structures service.

Acknowledgements

This work was supported by the NIGMS GM119426 (W.M.W.), 1F31AI191720-01 (A.R.L.), and T32GM152344 (J.R.S.). Research reported in this publication was supported by the National Institute of General Medical Sciences of the National Institutes of Health under award number T32GM152344. The content is solely the responsibility of the authors and does not necessarily represent the official views of the National Institutes of Health, Emory University, or the BDCI training program. The authors would like to thank Riley Hughes for his insightful discussions on cysteine reactivity.

References

(1) Newman, D. J.; Cragg, G. M. Natural Products as Sources of New Drugs over the Nearly Four Decades from 01/1981 to 09/2019. *J. Nat. Prod.* **2020**, *83* (3), 770–803. https://doi.org/10.1021/acs.jnatprod.9b01285.

(2) *COVID-19: U.S. Impact on Antimicrobial Resistance, Special Report 2022*; National Center for Emerging and Zoonotic Infectious Diseases, 2022. https://doi.org/10.15620/cdc:117915.

(3) Athena P. Kourtis; Kelly Hatfield; James Baggs; Yi Mu; Isaac See; Erin Epson; Joelle Nadle; Marion A. Kainer; Ghinwa Dumyati; Susan Petit; Susan M. Ray; David Ham; Catherine Capers; Heather Ewing; Nicole Coffin; L. Clifford McDonald; John Jernigan; Denise Cardo. *Vital Signs: Epidemiology and Recent Trends in Methicillin-Resistant and in Methicillin-Susceptible Staphylococcus Aureus Bloodstream Infections — United States*; Morbidity and Mortality Weekly Report; US Department of Health and Human Services/Centers for Disease Control and Prevention, 2019; pp 214–219. https://www.cdc.gov/mmwr/volumes/68/wr/pdfs/mm6809e1-H.pdf.

(4) Centers for Disease Control and Prevention (U.S.). *Antibiotic Resistance Threats in the United States, 2019*; Centers for Disease Control and Prevention (U.S.), 2019. https://doi.org/10.15620/cdc:82532.

(5) Veve, M. P.; Wagner, J. L. Lefamulin: Review of a Promising Novel Pleuromutilin Antibiotic. *Pharmacother. J. Hum. Pharmacol. Drug Ther.* **2018**, *38* (9), 935–946. https://doi.org/10.1002/phar.2166.

(6) Food and Drug Administration. Edward M. Cox. NDA Approval Letter: Xenleta (Lefamulin) (NDA 211672 211673), 2019. https://www.accessdata.fda.gov/drugsatfda_docs/appletter/2019/211672Orig1s000,%20211673Orig1s000ltr.pdf (accessed 2026-03-26).

(7) Falagas, M. E.; Fanariotis, G.; Romanos, L. T.; Katsikas, K. M.; Kakoullis, S. A. Resistance to Lefamulin: An Evaluation of Data from In Vitro Antimicrobial Susceptibility Studies. *Antibiotics* **2026**, *15* (1), 58. https://doi.org/10.3390/antibiotics15010058.

(8) Mellett, M.; Lawandi, A.; Caya, C.; Lee, T. C.; Babiker, A.; Papenburg, J.; Yansouni, C. P.; Cheng, M. P. Antibiotic Synergy against *Staphylococcus Aureus* : A Systematic Review and Meta-Analysis. *Antimicrob. Agents Chemother.* **2025**, *69* (8), e01199-24. https://doi.org/10.1128/aac.01199-24.

(9) Chen, Y.; Huang, H.-B.; Peng, J.-M.; Weng, L.; Du, B. Efficacy and Safety of Ceftazidime-Avibactam for the Treatment of Carbapenem-Resistant *Enterobacterales* Bloodstream Infection: A Systematic Review and Meta-Analysis. *Microbiol. Spectr.* **2022**, *10* (2), e02603-21. https://doi.org/10.1128/spectrum.02603-21.

(10) Takata, K.; Iwatsuki, M.; Yamamoto, T.; Shirahata, T.; Nonaka, K.; Masuma, R.; Hayakawa, Y.; Hanaki, H.; Kobayashi, Y.; Petersson, G. A.; Ōmura, S.; Shiomi, K. Aogacillins A and B Produced by *Simplicillium* Sp. FKI-5985: New Circumventors of Arbekacin Resistance in MRSA. *Org. Lett.* **2013**, *15* (18), 4678–4681. https://doi.org/10.1021/ol401975z.

(11) Gu, H.; Li, Z.; Zhang, X.; Sang, R.; Li, Z.; Ren, J.; Chen, X.; Ma, B.; Qiu, W.; Yang, Z.; Li, X.; Tong, R.; Zhang, W. Total Syntheses of *Ent* -Aogacillin A and Aogacillin B. *Chem. Sci.* **2026**, *17* (4), 2164–2168. https://doi.org/10.1039/D5SC04554A.

(12) Crossley, S. W. M.; Tong, G.; Lambrecht, M. J.; Burdge, H. E.; Shenvi, R. A. Synthesis of (−)-Picrotoxinin by Late-Stage Strong Bond Activation. *J. Am. Chem. Soc.* **2020**, *142* (26), 11376–11381. https://doi.org/10.1021/jacs.0c05042.

(13) Greiner, L. C.; Pahl, A.; Heinzke, A. L.; Zdrazil, B.; Leach, A. R.; Young, R. J.; Leeson, P. D.; Waldmann, H. Pseudonatural Products for Chemical Biology and Drug Discovery. *J. Med. Chem.* **2025**, *68* (14), 14137–14170. https://doi.org/10.1021/acs.jmedchem.5c00643.

(14) Truax, N. J.; Ayinde, S.; Liu, J. O.; Romo, D. Total Synthesis of Rameswaralide Utilizing a Pharmacophore-Directed Retrosynthetic Strategy. *J. Am. Chem. Soc.* **2022**, *144* (40), 18575–18585. https://doi.org/10.1021/jacs.2c08245.

(15) Truax, N. J.; Romo, D. Bridging the Gap between Natural Product Synthesis and Drug Discovery. *Nat. Prod. Rep.* **2020**, *37* (11), 1436–1453. https://doi.org/10.1039/D0NP00048E.

(16) Grigalunas, M.; Burhop, A.; Christoforow, A.; Waldmann, H. Pseudo-Natural Products and Natural Product-Inspired Methods in Chemical Biology and Drug Discovery. *Curr. Opin. Chem. Biol.* **2020**, *56*, 111–118. https://doi.org/10.1016/j.cbpa.2019.10.005.

(17) Li, C.; Shenvi, R. A. Total Synthesis of 25 Picrotoxanes by Virtual Library Selection. *Nature* **2025**, *638* (8052), 980–986. https://doi.org/10.1038/s41586-024-08538-y.

(18) Solinski, A. E.; Koval, A. B.; Brzozowski, R. S.; Morrison, K. R.; Fraboni, A. J.; Carson, C. E.; Eshraghi, A. R.; Zhou, G.; Quivey, R. G.; Voelz, V. A.; Buttaro, B. A.; Wuest, W. M. Diverted Total Synthesis of Carolacton-Inspired Analogs Yields Three Distinct Phenotypes in *Streptococcus Mutans* Biofilms. *J. Am. Chem. Soc.* **2017**, *139* (21), 7188–7191. https://doi.org/10.1021/jacs.7b03879.

(19) Gennaiou, K.; Zografos, A. L. Oxidation-Induced Scaffold Remodeling in *Ainsliaea* Disesquiterpenoids: Total Synthesis of Macrocephadiolide A. *Org. Lett.* **2026**, acs.orglett.6c00658. https://doi.org/10.1021/acs.orglett.6c00658.

(20) Dong, J.-W.; Cai, L.; Li, X.-J.; Mei, R.-F.; Wang, J.-P.; Luo, P.; Shu, Y.; Ding, Z.-T. Fermentation of Illigera Aromatica with Clonostachys Rogersoniana Producing Novel Cytotoxic Menthane-Type Monoterpenoid Dimers. *RSC Adv.* **2017**, *7* (62), 38956–38964. https://doi.org/10.1039/C7RA06078E.

(21) Zhang, Y.; Lu, Y.; Mao, L.; Proksch, P.; Lin, W. Tagalsins I and J, Two Novel Tetraterpenoids from the Mangrove Plant, *Ceriops t Agal*. *Org. Lett.* **2005**, *7* (14), 3037–3040. https://doi.org/10.1021/ol0509843.

View Article Online
DOI: 10.1039/D6SC04046B

(22) Böttcher, T. An Additive Definition of Molecular Complexity. *J. Chem. Inf. Model.* **2016**, *56* (3), 462–470. https://doi.org/10.1021/acs.jcim.5b00723.
(23) Shenvi, R. A. Natural Product Synthesis in the 21st Century: Beyond the Mountain Top. *ACS Cent. Sci.* **2024**, *10* (3), 519–528. https://doi.org/10.1021/acscentsci.3c01518.
(24) Demoret, R. M.; Baker, M. A.; Ohtawa, M.; Chen, S.; Lam, C. C.; Khom, S.; Roberto, M.; Forli, S.; Houk, K. N.; Shenvi, R. A. Synthetic, Mechanistic, and Biological Interrogation of *Ginkgo Biloba* Chemical Space En Route to (−)-Bilobalide. *J. Am. Chem. Soc.* **2020**, *142* (43), 18599–18618. https://doi.org/10.1021/jacs.0c08231.
(25) Woo, S.; Landwehr, E. M.; Shenvi, R. A. Synthesis of Psychotropic Alkaloids from Galbulimima. *Tetrahedron* **2022**, *126*, 133064. https://doi.org/10.1016/j.tet.2022.133064.

View Article Online
DOI: 10.1039/D6SC04046B

The data underlying this study are available in the published article and its Supporting Information.

The data underlying this study are available in the published article and its Supporting Information. Detailed experimental procedures, characterization data, and NMR spectra. Compound **8** corresponds to CCDC accession code 2541815. Compound **9** corresponds to CCDC accession code 2541841. Compound **12** corresponds to CCDC accession code 2543179. Compound corresponds **25** to CCDC accession code 2547911. Compound **29** corresponds to CCDC accession code 2549876.These data can be obtained free of charge via the joint Cambridge Crystallographic Data Centre (CCDC) and Fachinformationszentrum Karlsruhe Access Structures service.